Supporting Information

Insights into the effective inhibition of green oil formation on the PdMo bimetallic catalyst in the selective hydrogenation of acetylene

Ning He[a], Junqi Pei[a], Zixuan Zhang[b], Ruijun Hou[a*]

a. Beijing Key Laboratory of Green Hydrogen and Fuel Cells, School of Chemistry and Chemical Engineering, Beijing Institute of Technology, Beijing, 100081, People's Republic of China.

b. Daqing Huakai Petrochemical Design & Engineering Co. Ltd, Heilongjiang, People's Republic of China

Contents

1. Methods

1.1 Volume change

1.2 Iteration method

1.3 Characterization details

2. Supplementary tables

Table S1. Apparent activation energies of the investigated catalysts

Table S2. Bader Charge for C_2H_2 Stabilized Adsorption on Pd(111) and Pd_1Mo_1(111) Surfaces.

Table S3. Bader Charge for C_2H_4 Stabilized Adsorption on Pd(111) and Pd_1Mo_1(111) Surfaces.

Table S4. Average Bader charge analysis for the stable adsorption of C_2H_2 and C_2H_4.

Table S5. Activation barriers of the two most probable 1,3-butadiene formation pathways.

3. Supplementary figures

Figure S1. TEM images at 20 nm of (a) Pd/SiO_2, (b) Pd_3Mo_1/SiO_2, (c) Pd_1Mo_1/SiO_2, (d)Pd_1Mo_3/SiO_2.

Figure S2. EDS elemental mapping of the unsupported nanoparticles: (a_1-a_3) Pd/SiO_2, (b_1-b_4) Pd_3Mo_1/SiO_2, (c_1-c_4) Pd_3Mo_1/SiO_2 and (d_1-d_4) Pd_1Mo_3/SiO_2.

Figure S3. Product selectivities at the different temperatures in acetylene hydrogenation: (a) ethylene, (b) ethane, and (c) green oil. (C_2H_2 : H_2 : N_2= 1:3:4; GHSV = 60000 mL g^{-1} h^{-1}).

Figure S4. TOFs normalized by surface sites over the investigated catalysts. (C_2H_2 : H_2 : N_2= 1:3:4; GHSV = 60000 mL g^{-1} h^{-1}).

Figure S5. Product selectivities as a function of acetylene conversion: (a) C_4, (b) C_{6+} and (c) oligomer. (C_2H_2 : H_2 : N_2= 1:3:4; GHSV = 60000 mL g^{-1} h^{-1})

Figure S6. The optimized configurations of transition states involved in the acetylene hydrogenation on (a) Pd(111) and (b) Pd_1Mo_1(111) surfaces.

Figure S7. The optimized configurations of transition states involved in the acetylene dimerization reaction on (a) Pd(111) and (b) Pd_1Mo_1(111) surfaces.

1. Methods

1.1 Volume change

Volume change cannot be neglected in the high-concentration acetylene feed. Therefore, carbon balance is calculated based on the main reactions involved in acetylene hydrogenation. The produced green oil is assumed as alkene for simplification.

a) $C_2H_2 + H_2 \rightarrow C_2H_4$;

b) $C_2H_2 + 2H_2 \rightarrow C_2H_6$;

c) $2C_2H_2 + H_2 \rightarrow C_4H_6$ (1,3-butadiene)

d) $2C_2H_2 + 2H_2 \rightarrow C_4H_8$ (butenes)

e) $2C_2H_2 + 3H_2 \rightarrow C_4H_{10}$ (butanes)

f) $3C_2H_2 + 2H_2 \rightarrow C_6H_{10}$ (C6+)

g) $C_2H_2 + H_2 \rightarrow 2/nC_nH_{2n}$ (Green oil, liquid)

If the inlet gas composition is C_2H_2:H_2:N_2=1:3:4, the acetylene proportion of the inlet is 1/8.

With the conversion *X*, 1mol acetylene takes up the amount of hydrogen of

$$X \cdot S_{C_2H_4} + 2X \cdot S_{C_2H_6} + \frac{1}{2}X \cdot S_{C_4H_6} + X \cdot S_{C_4H_8} + \frac{3}{2}X \cdot S_{C_4H_{10}} + \frac{2}{3}X \cdot S_{C_6H_{10}} + X \cdot S_{GO} \quad \text{(S1)}$$

and produces the amount of gaseous carbon species of

$$1 - \frac{1}{2}X \cdot S_{C_4H_6} - \frac{1}{2}X \cdot S_{C_4H_8} - \frac{1}{2}X \cdot S_{C_4H_{10}} - \frac{2}{3}X \cdot S_{C_6H_{10}} - X \cdot S_{GO} \quad \text{(S2)}$$

Therefore, the total amount of gas after the reaction for each mole of inlet acetylene is

$$8 - X \cdot S_{C_2H_4} - 2X \cdot S_{C_2H_6} - X \cdot S_{C_4H_6} - \frac{3}{2}X \cdot S_{C_4H_8} - 2X \cdot S_{C_4H_{10}} - \frac{4}{3}X \cdot S_{C_6H_{10}} - 2X \cdot S_{GO} \quad \text{(S3)}$$

with the acetylene content at the outlet

$$\frac{1 - \frac{1}{2}X \cdot S_{C_4H_6} - \frac{1}{2}X \cdot S_{C_4H_8} - \frac{1}{2}X \cdot S_{C_4H_{10}} - \frac{2}{3}X \cdot S_{C_6H_{10}} - X \cdot S_{GO}}{8 - X \cdot S_{C_2H_4} - 2X \cdot S_{C_2H_6} - X \cdot S_{C_4H_6} - \frac{3}{2}X \cdot S_{C_4H_8} - 2X \cdot S_{C_4H_{10}} - \frac{4}{3}X \cdot S_{C_6H_{10}} - 2X \cdot S_{GO}} \quad \text{(S4)}$$

By using the above equation, the volume change is incorporated into the external method.

1.2 Iteration method

The iteration method includes the following steps:

(1) Denote the inlet molar flow rate of hydrocarbon gas as C_0, and the total flow rate of the inlet gas as N_0. The inlet hydrocarbon proportion is calculated as $\alpha_0 = C_0 / N_0$.

(2) The inlet acetylene peak area observed from the GC chromatogram is denoted as A_0.

(3) The outlet gas is analyzed by GC, and the peak areas of the detected species are denoted as A_i, with the correction factor denoted as f_i.

(4) The initial guess of the conversion (X) and selectivities (S_i) to the detected species are calculated by the internal method.

$$X = 1 - \frac{A_{C_2H_2} * f_{C2H2}}{\Sigma A_i * f_i} \quad \text{(S5)}$$

$$S_i = \frac{A_i * f_i}{\Sigma A_i * f_i - A_{C_2H_2} * f_{C2H2}} \quad \text{(S6)}$$

(5) The total gas change (ΔN) and the hydrocarbon gas change (ΔC) are calculated by the initial guess, and the outlet hydrocarbon proportion (α) could be roughly calculated.

$$\Delta C = \sum \beta_i * S_i * X \quad \text{(S7)}$$

$$\Delta N = \sum \gamma_i * S_i * X \quad \text{(S8)}$$

$$\alpha = (C_0 + \Delta C)/(N_0 + \Delta N) \quad \text{(S9)}$$

where β_i is the molar change of gaseous hydrocarbon with 1 mol C_2H_2 reacted to species i, γ_i is the total molar change of gas with 1 mol C_2H_2 reacted to species i.

(6) The convergence factor is defined as $\kappa_0 = \alpha_0/\alpha$. Let k =1.

(7) The peak areas are corrected by the convergence factor $\kappa_{k-1} * A_i * f_i$, and the kth corrected conversion and selectivities could be obtained.

$$X = 1 - \frac{\kappa_{k-1} * A_{C_2H_2}}{A_0} \quad \text{(S10)}$$

$$S_i = \frac{\kappa_{k-1} * A_i * f_i}{(A_0 - \kappa_{k-1} * A_{C_2H_2}) * f_{C2H2}} \quad \text{(S11)}$$

$$S_{GO} = 1 - \sum S_i \quad \text{(S12)}$$

where S_{GO} is the green oil selectivity.

(8) The total gas change (ΔN) and the hydrocarbon gas change (ΔC) are calculated by the kth correction according to Step (5), and the outlet hydrocarbon proportion(α) could be roughly calculated by Eq (S9).

(9) The kth convergence factor is calculated by $\kappa_k = \alpha_0/\alpha_k$.

(10) If $|\kappa_k - \kappa_{k-1}|$ is lower than the convergence criteria, the iteration is ended; if not, let $k=k+1$, return to step (7).

1.3 Characterization details

The lattice distance, lattice parameters, and crystalline size in Table 1 were calculated using Bragg's law (Eq (S13)), the Scherrer equation (Eq (S14)), and Eq (S15) using the data at the Pd(111) crystal plane on the XRD profiles.

$$d_{(111)} = \frac{\mathrm{n}\lambda}{2\sin\theta_{(111)}} \tag{S13}$$

$$D_{(111)} = \frac{\mathrm{K}\lambda}{\beta_{(111)}cos\theta_{(111)}} \tag{S14}$$

$$a(111) = \frac{\sqrt{3}n\lambda}{2sin\theta_{(111)}} \tag{S15}$$

Where, $d_{(111)}$is the lattice distance of the (111) crystal plane, $D_{(111)}$ is the average crystalline size, $a_{(111)}$is the lattice parameter, n is the diffraction order, λ is the wavelength (0.154 nm) of the electromagnetic wave generated by the electron beam bombarding the Cu target, θ is the diffraction angle, K is the Scherrer constant (0.89), and β is the half-width of the diffraction peak.

The La values in Table 4 were calculated using the Tuinstra-Koenig equation:

$$\frac{I_D}{I_G} = \frac{C(\lambda)}{L_a} \tag{S16}$$

where I_D and I_G are the intensities of the D band and G band, respectively, C (515.5 nm) is approximately 4.4 nm. The L_a value indicates the relative proportion of ordered graphitic structures within the deposited carbon on the catalyst surface. A higher value implies a greater degree of ordered graphitization in the deposited carbon.

2. Supplementary tables

Table S1 Apparent activation energies of the investigated catalysts

Catalyst	Apparent activation energy ($kJ \cdot mol^{-1}$)
Pd/SiO_2	60.4
Pd_3Mo_1/SiO_2	48.3
Pd_1Mo_1/SiO_2	46.5
Pd_1Mo_3/SiO_2	47.2

Table S2 Bader charge for C_2H_2 stabilized adsorption on Pd(111) and Pd_1Mo_1(111) surfaces

No.	Pd(111)		Pd_1Mo_1(111)	
	Element	charges	Element	charges
1	Pd	-0.003239	Pd	-0.001295
2	Pd	-0.005759	Pd	-0.002380
3	Pd	-0.005384	Pd	0.001290
4	Pd	-0.006156	Pd	-0.003531
5	Pd	-0.013275	Pd	0.018221
6	Pd	-0.011743	Pd	0.023730
7	Pd	-0.007191	Mo	-0.002288
8	Pd	-0.007830	Mo	-0.004090
9	Pd	-0.047973	Mo	-0.007090
10	Pd	0.084174	Mo	-0.006966
11	Pd	0.048786	Mo	0.027334
12	Pd	0.046407	Mo	0.022939
13	C	-0.024290	C	-0.032266
14	C	-0.043909	C	-0.027381
15	H	-0.002350	H	-0.002735
16	H	-0.000267	H	-0.003491

Table S3 Bader charge for C_2H_4 stabilized adsorption on Pd(111) and Pd_1Mo_1(111) surfaces

No.	Pd(111)		Pd_1Mo_1(111)	
	Element	charges	Element	charges
1	Pd	-0.002099	Pd	-0.002469
2	Pd	-0.002640	Pd	-0.002589
3	Pd	-0.004315	Pd	-0.003489
4	Pd	-0.004896	Pd	0.000558
5	Pd	-0.009660	Pd	-0.018287
6	Pd	-0.008806	Pd	-0.007887
7	Pd	-0.005312	Mo	0.001232
8	Pd	-0.005098	Mo	-0.000623
9	Pd	-0.012511	Mo	-0.007866
10	Pd	-0.021350	Mo	-0.004618
11	Pd	0.041957	Mo	0.040194
12	Pd	0.042285	Mo	0.011444
13	C	0.016205	C	0.029121
14	C	-0.021503	C	-0.033705
15	H	-0.000630	H	-0.000310
16	H	-0.000360	H	-0.000335
17	H	-0.000908	H	-0.000371
18	H	-0.000346	H	0

Table S4 Average Bader charge analysis for the stable adsorption of C_2H_2 and C_2H_4

charge	Pd(111)		Pd_1Mo_1(111)	
transferred/eV	Pd	——	Pd	Mo
C_2H_2	0.071	——	0.042	0.050
C_2H_4	0.050	——	-0.011	0.052

Table S5 Activation barriers of the two most probable 1,3-butadiene formation pathways

Pathway I	TS1-1 C_2H_2+H	TS3 C_2H_2+C_2H_3	TS5 C_4H_5+H
Pd(111)	0.97	0.92	0.78
Pd1Mo1(111)	1.33	1.04	1.41
Pathway II	**TS1-1 C_2H_2+H**		**TS4 C_2H_3+C_2H_3**
Pd(111)	0.97		0.89
Pd1Mo1(111)	1.33		1.10

3. Supplementary figures

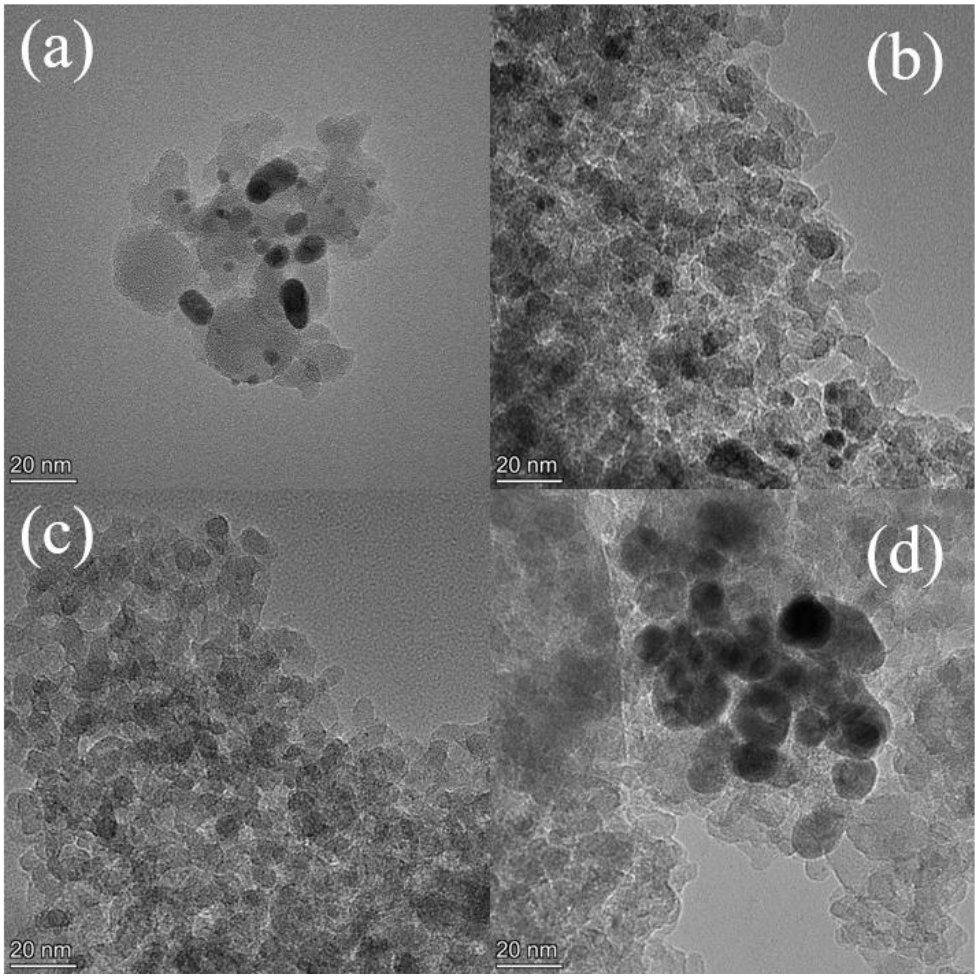

Figure S1 TEM images at 20 nm of (a) Pd/SiO_2, (b) Pd_3Mo_1/SiO_2, (c) Pd_1Mo_1/SiO_2, (d)Pd_1Mo_3/SiO_2

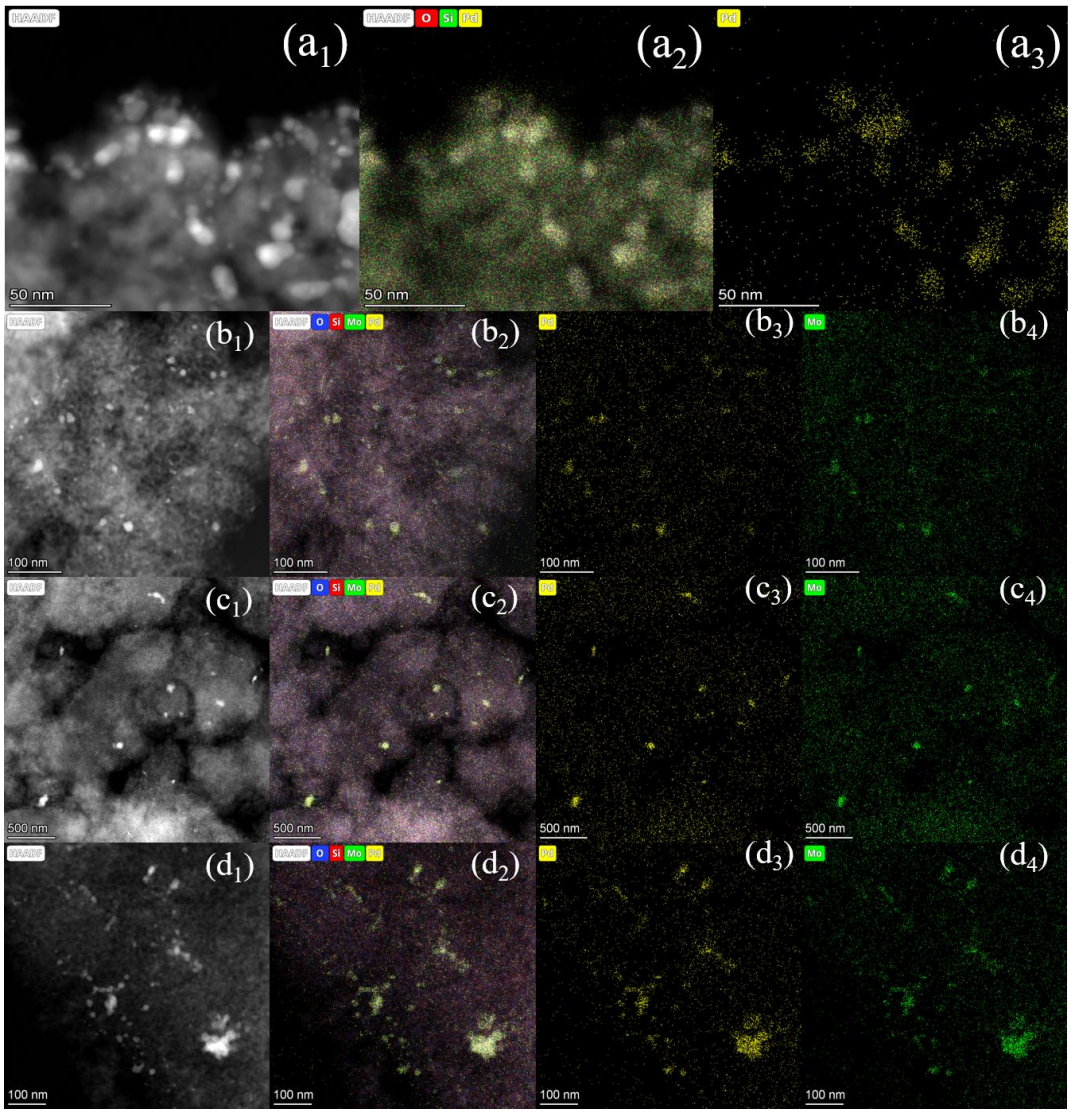

Figure S2 EDS elemental mapping of the unsupported nanoparticles:

(a_1-a_3) Pd/SiO_2, (b_1-b_4) Pd_3Mo_1/SiO_2, (c_1-c_4) Pd_3Mo_1/SiO_2 and (d_1-d_4) Pd_1Mo_3/SiO_2

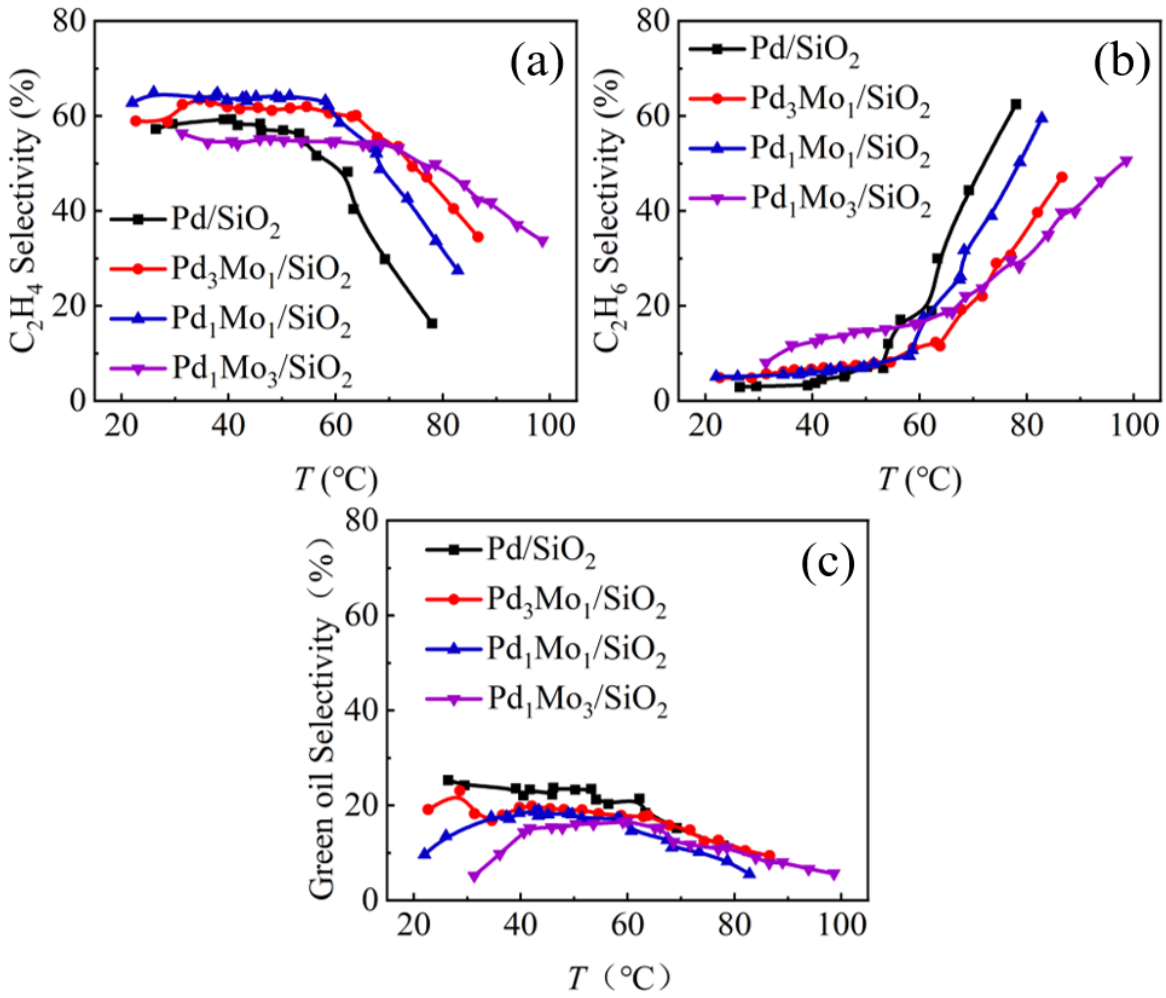

Figure S3 Product selectivities at the different temperatures in acetylene hydrogenation:

(a) ethylene, (b) ethane, and (c) green oil. (C_2H_2 : H_2 : N_2 = 1:3:4; GHSV = 60000 mL g^{-1} h^{-1}).

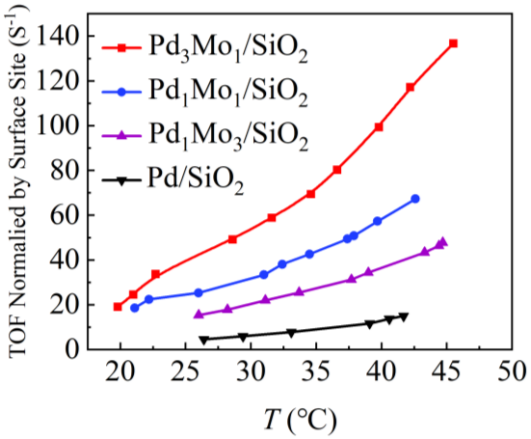

Figure S4 TOFs normalized by surface sites over the investigated catalysts.

(C_2H_2 : H_2 : N_2 = 1:3:4; GHSV = 60000 mL g^{-1} h^{-1}).

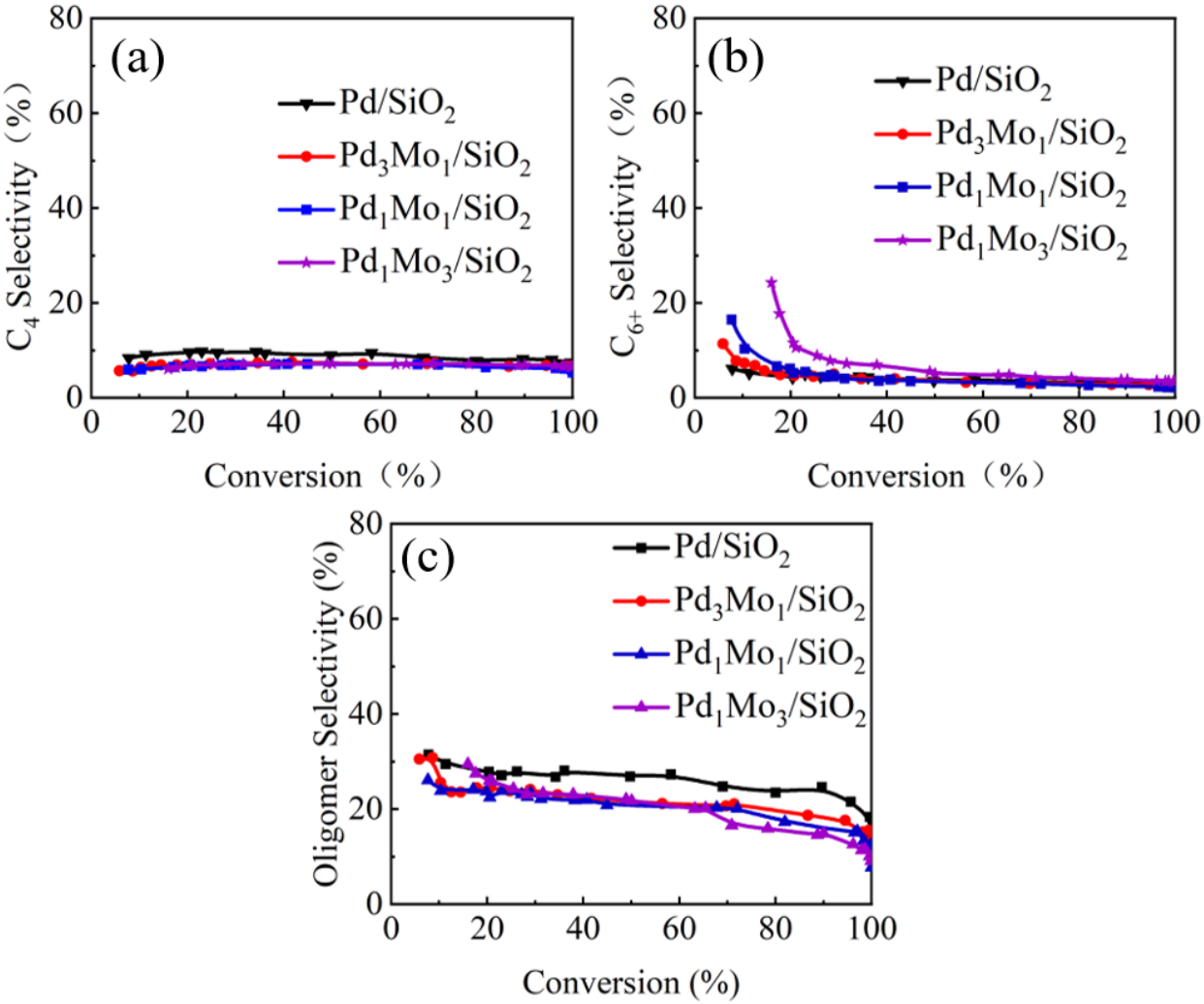

Figure S5 Product selectivities as a function of acetylene conversion:

(a) C_4, (b) C_{6+} and (c) oligomer. (C_2H_2 : H_2 : N_2= 1:3:4; GHSV = 60000 mL g^{-1} h^{-1})

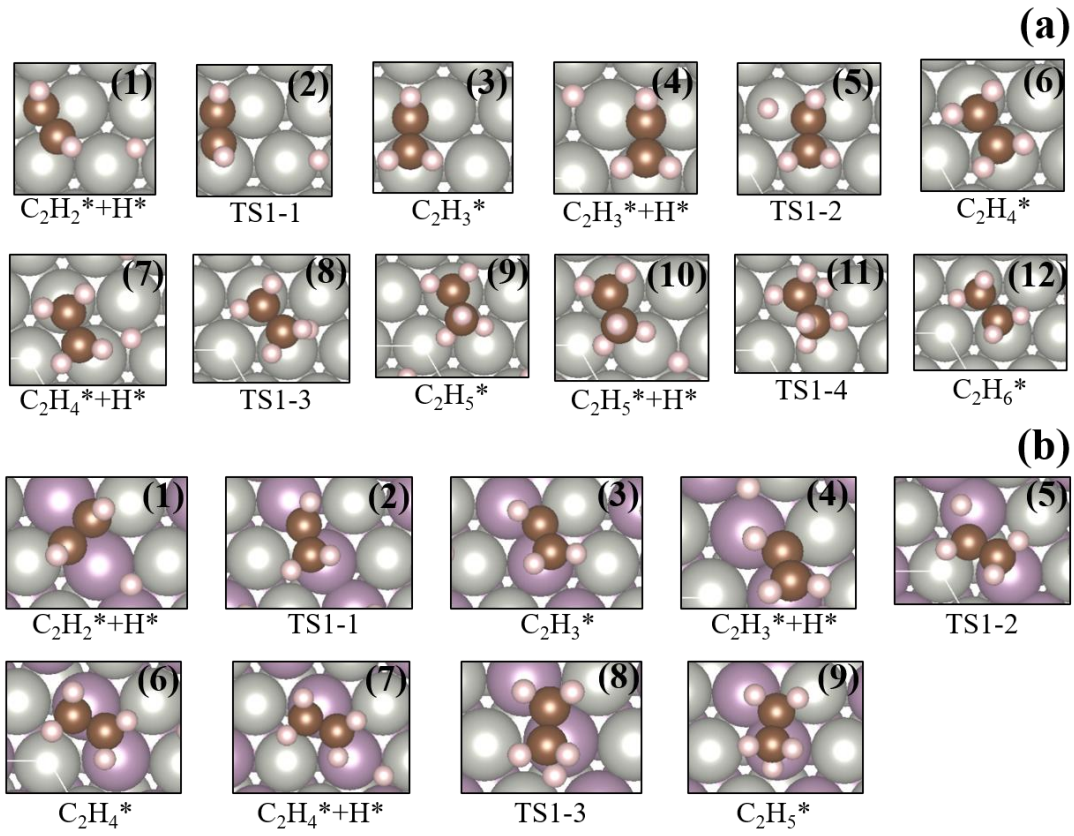

Figure S6 The optimized configurations of transition states involved in the acetylene hydrogenation on (a) Pd(111) and (b) Pd_1Mo_1(111) surfaces.

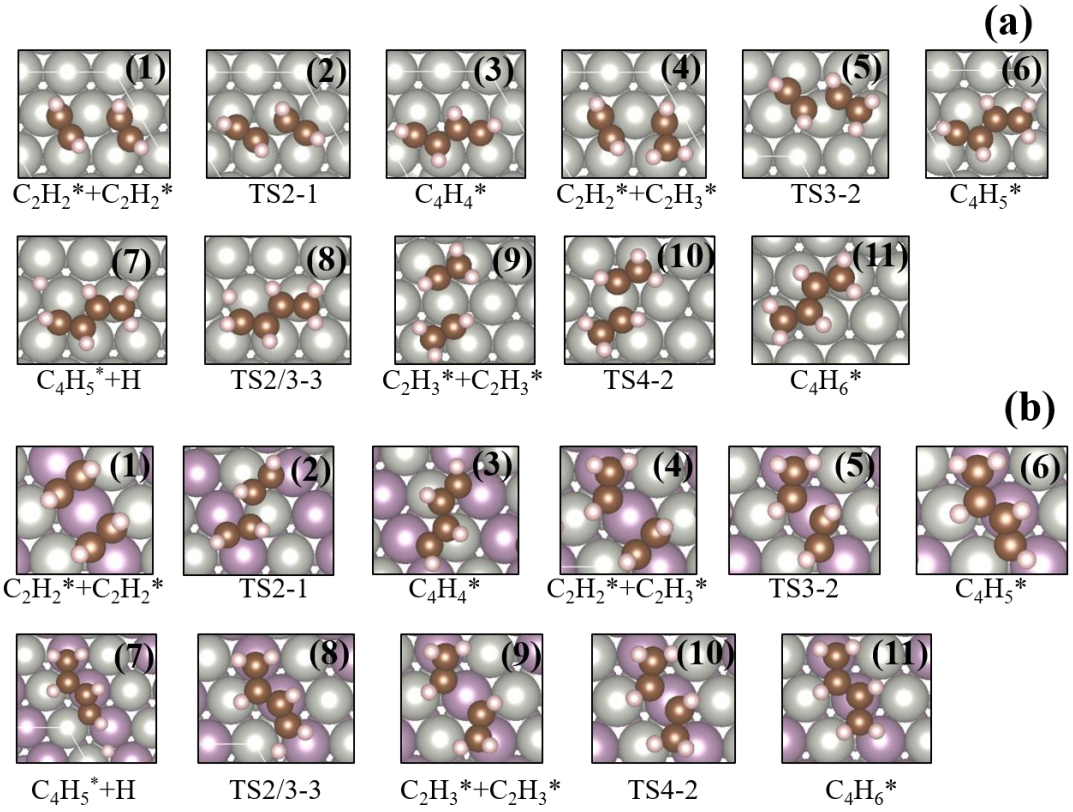

Figure S7 The optimized configurations of transition states involved in the acetylene dimerization reaction on (a) Pd(111) and (b) Pd_1Mo_1(111) surfaces.

References

[1] G. Kresse, J. Furthmüller, Efficient iterative schemes for ab initio total-energy calculations using a plane-wave basis set, Phys. Rev. B 54 (16) (1996) 11169.

[2] G. Kresse, D. Joubert, From ultrasoft pseudopotentials to the projector augmented-wave method, Phys. Rev. B 59 (3) (1999) 1758.

[3] J. P. Perdew, K. Burke, Ernzerhof, M., Generalized gradient approximation made simple, Phys. Rev. Lett. 77 (18) (1996) 3865.

[4] H. J. Monkhorst, J. D. Pack, Special points for Brillouin-zone integrations, Phys. Rev. B 13 (12) (1976) 5188.

[5] S. Grimme, J. Antony, S. Ehrlich, H. Krieg, A consistent and accurate ab initio parametrization of density functional dispersion correction (DFT-D) for the 94 elements H-Pu, J. Chem. Phys. 132 (15) 2010 154104.